Topoisomerase IV Bends and Overtwists DNA upon Binding

G. Charvin,*† T. R. Strick,‡ D. Bensimon,* and V. Croquette*
*Laboratoire de Physique Statistique, Ecole Normale Supérieure, UMR 8550 Centre National de la Recherche Scientifique, Paris, France; †The Rockefeller University, New York, New York; and ‡Institut Jacques Monod, Paris, France

ABSTRACT *Escherichia coli* topoisomerase IV (Topo IV) is an essential ATP-dependent enzyme that unlinks sister chromosomes during replication and efficiently removes positive but not negative supercoils. In this article, we investigate the binding properties of Topo IV onto DNA in the absence of ATP using a single molecule micromanipulation setup. We find that the enzyme binds cooperatively (Hill coefficient $\alpha \sim 4$) with supercoiled DNA, suggesting that the Topo IV subunits assemble upon binding onto DNA. It interacts preferentially with (+) rather than (−) supercoiled DNA ($K_d^+ = 0.15$ nM, $K_d^- = 0.23$ nM) and more than two orders-of-magnitude more weakly with relaxed DNA ($K_d^0 \sim 36$ nM). Like gyrase but unlike the eukaryotic Topo II, Topo IV bends DNA with a radius $R_0 = 6.4$ nm and locally changes its twist and/or its writhe by 0.16 turn per bound complex. We estimate its free energy of binding and study the dynamics of interaction of Topo IV with DNA at the binding threshold. We find that the protein/DNA complex alternates between two states: a weakly bound state where it stays with probability $p = 0.89$ and a strongly bound state (with probability $p = 0.11$). The methodology introduced here to characterize the Topo IV/DNA complex is very general and could be used to study other DNA/protein complexes.

INTRODUCTION

Topoisomerases are enzymes responsible for the regulation of DNA topology in the cell (1,2). Type II topoisomerases catalyze the ATP-dependent passage of one DNA segment (the transport, or T-segment) through another (the gate, or G-segment). They decatenate sister chromosomes during DNA replication (3) and are known to regulate the level of supercoiling during replication, transcription, and recombination (4).

Prokaryotes possess two structurally similar type II topoisomerases, Gyrase and Topo IV, which differ in their function. Gyrase generates negative supercoiling (5), which promotes the compaction of DNA and regulates transcription (6). Topo IV is known to play a critical role during DNA replication: it removes positive supercoils generated downstream from the replication complex (7) and may unlink the newly synthesized sister chromosomes (8,7). Whereas eukaryotic type II topoisomerases are able to relax both positively ((+)scDNA) and negatively ((−)scDNA) supercoiled DNA, Topo IV has been shown to relax preferentially (+)scDNA (9). Since Topo IV binds (−)scDNA with the same efficiency as (+)scDNA (10), this chiral discrimination is unlikely at the level of enzymatic binding. Instead, it might be due to the relative orientation of the T- and G-segments, which is different in (+)scDNA and (−)scDNA supercoils (9–11). Nevertheless, unraveling the geometry of interaction of DNA with Topo IV is important for understanding its mechanism. Electron microscopy images of Topo IV suggested that the enzyme bends DNA (12), and that DNA cyclization assays in the presence of Topo IV (12) could be fitted assuming a bending radius of 7 nm. Recent crystallographic studies (13) of the Gyrase and Topo IV C-terminal regions have also found the DNA to be bent with a radius $R \sim 6$ nm. However, the cyclization data could be fitted with a purely bent untwisted DNA molecule, which is a bit surprising since previous experiments reported a small induction of (+)supercoils in DNA upon binding to Topo IV (14) and since Gyrase is known to bend DNA into a tight right-handed solenoidal form (15).

In the following, we describe a quantitative and systematic investigation of Topo IV/DNA interactions in the absence of ATP, using a single DNA micromanipulation setup based on a magnetic trap (16,17). We show that the interaction is strongly cooperative (Hill coefficient $\alpha \sim 4$) and saturates at concentrations of Topo IV $\approx$ 0.3 nM. As previously reported, Topo IV appears to strongly bend supercoiled DNA, thereby changing the characteristic dimensions of its interwound supercoiled structures. However, in contrast with cyclization experiments, we find that Topo IV binding to DNA induces local changes in its twist ΔTw and/or its writhe ΔWr such that $\Delta \equiv \Delta Wr + \Delta Tw = 0.16$ per enzyme/DNA complex.

A simple mechanical model is capable of explaining the observed force- and supercoiling-dependence of the interaction. From this model, we extract the radius of curvature that the enzyme imposes on the DNA, $R_0 \approx 6.4$ nm, and estimate the free energy of binding, $\Delta G^{\sigma>0}_{\text{binding}} \approx -12\,k_BT$ on (+)scDNA and $\Delta G^{0}_{\text{binding}} \approx 10\,k_BT$ on relaxed DNA (at [Topo IV] = 3 nM). A study of the dynamics of Topo IV binding reveals the existence of two states with different timescales, which suggest the existence of two bound conformations with distinct lifetimes. This study illuminates some of the similarities and differences in the topoisomerase/DNA complex in eukaryotes and prokaryotes. It supports the

Submitted January 26, 2005, and accepted for publication April 27, 2005.

Address reprint requests to Gilles Charvin, E-mail: gcharvin@rockefeller.edu.

0006-3495/05/07/384/09 $2.00

doi: 10.1529/biophysj.105.060202

idea that the Gyrase and Topo IV binding mechanisms are structurally related. Finally, the general experimental and theoretical methodology used here could be similarly applied to investigate the binding of other proteins onto DNA.

MATERIALS AND METHODS

DNA constructs and micromanipulation setup

We multipally labeled 17-kbp, 11-kbp, and 3-kbp DNAs at their extremities with biotin and digoxigenin (DIG) as previously described (17). The molecules were bound at one end to a streptavidin-coated magnetic bead (2.8 μm or 1 μm; Dynal Biotech, Invitrogen, Lake Success, NY) and at the other to a glass surface coated with anti-DIG and passivated with BSA (Roche, Basel, Switzerland). We translated small magnets placed above the sample to set the force pulling on the bead and rotated them to apply a torsional stress on the DNA. Bead tracking and force F measurement were performed on an inverted microscope (16) (F was measured with 10% accuracy). The extension z was measured by tracking the three-dimensional position of the tethered bead in real-time at 25 Hz (17). In our experiments, the error on z was ~2 nm on a 3-kbp construct at $F = 2$ pN, averaging over 1 s (the error increases at lower force and for longer molecules).

Binding assays

Binding experiments with Topo IV (gift of N. Cozzarelli and N. Crisona) were performed at 25°C in 25 mM Tris buffer (pH = 7.6) containing 100 mM potassium glutamate, 10 mM $MgCl_2$, 0.5 mM dithiothreitol, 50 μg/ml BSA (9).

Analyzing the dynamics of binding

We assume that the DNA/Topo IV complex exists in two distinct and sequential bound states denoted *1* and *2*. We denote by *0* the unbound state and by k_{-1}, k_2, and k_{-2} the rate constants associated with the kinetic steps shown in Fig. 5 *b*).

The probability $P(\tau > t)$ that the lifetime τ of the bound state is greater than t can be computed easily by solving the following set of ordinary differential equations,

$$\begin{aligned}\frac{dP_2}{dt} &= k_2P_1 - k_{-2}P_2\\ \frac{dP_1}{dt} &= -(k_{-1}+k_2)P_1 + k_{-2}P_2\\ \frac{dP_0}{dt} &= k_{-1}P_1,\end{aligned} \tag{1}$$

where $P_0(t)$, $P_1(t)$, and $P_2(t)$ are the probabilities of being in states *0*, *1*, and *2* at time t. The value $P(\tau > t)$ can be computed by remarking that $P(\tau > t) = 1 - P_0(t)$.

The solution of Eq. 1 with initial conditions $P_0(0) = P_2(0) = 0$ and $P_1(0) = 1$ yields

$$P(\tau > t) = \frac{k_{-1}+\lambda_-}{\lambda_- - \lambda_+}e^{\lambda_+ t} - \frac{\lambda_+ + k_{-1}}{\lambda_- - \lambda_+}e^{\lambda_- t} \tag{2}$$

with

$$\lambda_\pm = -\frac{1}{2}\left(k_{-1}+k_2+k_{-2} \pm \sqrt{(k_{-1}+k_2+k_{-2})^2 - 4k_{-1}k_{-2}}\right). \tag{3}$$

A best fit by a double exponential $P(\tau > t) = \alpha e^{\lambda_+ t} + (1-\alpha)e^{\lambda_- t}$ of the experimental data yields $\lambda_+ = -0.53$, $\lambda_- = -0.12$, and $\alpha = 0.89$, from which we extract the kinetic parameters $k_{-1} = 0.48 \pm 0.03\ s^{-1}$, $k_{-2} = 0.14 \pm 0.01\ s^{-1}$, and $k_2 = 0.03 \pm 0.01\ s^{-1}$.

To confirm the validity of our analysis, we have performed a stochastic numerical simulation of the dynamics of the kinetic pathway described in Fig. 5 *b*). Starting from state *1*, we let the system evolve randomly with transition probabilities given by the kinetic parameters (extracted from the experiments) and measure the time required to reach the unbound state. The results obtained after 10,000 such trials are reported in Fig. 5 *b*) and agree very well with the experimental data.

RESULTS

Testing the binding of topoisomerases to the G- and T-segments

In these experiments, a single 17-kbp DNA molecule (linking number $Lk_0 = 1600$; contour length $L = 5.8$ μm) was anchored at one extremity to the surface of a glass capillary, whereas the other end was bound to a superparamagnetic bead (see Fig. 1). The bead, pulled by the magnetic field gradient generated by small magnets, stretched the tethering molecule. Rotating the magnets by n turns allows us to change the supercoiling density $\sigma \equiv \Delta Lk/Lk0 = n/Lk_0$ of the DNA molecules, provided they are not nicked (16,17).

To investigate the interaction of Topo IV with DNA, we first examined whether, in the absence of ATP, the enzyme was capable of simultaneously binding the G- and T-segments present in interwound plectonemic structures, as had been previously observed in electron microscopy images of eukaryotic Topo II (18). To that end, an scDNA ($\sigma = 0.04$) was alternatively subjected to low ($F = 0.3$ pN) and

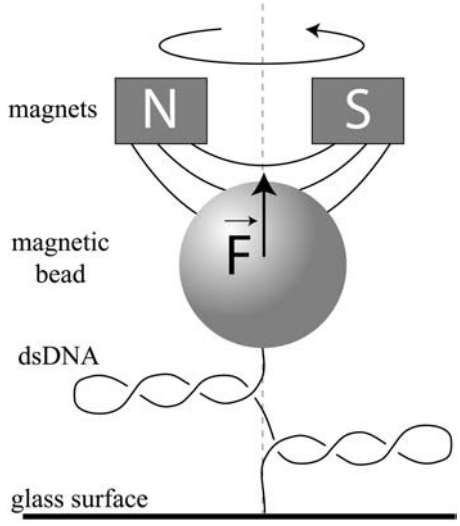

FIGURE 1 Sketch of the experimental setup. A single DNA molecule is multipally tagged at its extremities with biotin (*BIOT*) and digoxygenin (*DIG*), so that it can be attached to a streptavidin-coated superparamagnetic bead and an anti-DIG-coated glass surface. Translation and rotation of small magnets close to the DNA molecule (few mm) change, respectively, the force applied on it and the supercoiling density. The extension of the DNA is measured by tracking the position of the bead using an inverted microscope (see Materials and Methods for details).

high ($F = 5$ pN) stretching forces while its extension was monitored. By suddenly increasing the stretching force (the time required to change the force is <0.1 s), in absence of proteins, the DNA's extension increased in a rapid, smooth, and reproducible fashion (19) as supercoils were pulled out (Fig. 2 *a*).

This behavior is altered by the introduction of an enzyme such as eukaryotic Topo II which can bind to two DNA segments. Upon increasing the force, supercoils are removed rapidly, allowing the extension to grow, until a protein clamp is reached. The DNA's extension ceases to increase and a transient plateau is observed well below the maximal extension expected at that force (in 89% of the cases, i.e., out of 51 recorded) for the whole duration of the pull, i.e., ~ 40 s, see Fig. 2, *b* and *e*). If and when the protein clamp dissociates, downstream supercoils are suddenly exposed to the force and pulled out, leading to a jump in the DNA's extension. This characteristic pattern of plateaus and jumps is observed using *Drosophila melanogaster* Topo II demonstrating that this enzyme simultaneously binds to the G- and T-segments and stabilizes plectonemic supercoils (19).

The same experiment was performed with *Escherichia coli* Topo IV ([Topo IV] = 0.7 nM > K_d, see below) on (+)scDNA ($\sigma = \pm 0.04$). In contrast with the signal observed in presence of the eukaryotic enzyme, only 43% of events (out of 44 recorded) exhibit plateaus very near the maximal extension, which are almost always (95% of cases) released within 40 s (compare Fig. 2, *b* and *c*, and see Fig. 2 *e*). Namely, upon increasing the force, the DNA quickly recovers its maximal extension. These results indicate that, in contrast with Topo II, Topo IV weakly binds to the G- and T-segments in (+)scDNA crossings. On (−)scDNA, no clamping effect is observed at all, suggesting that the Topo IV interaction with DNA may be sensitive to the supercoiling chirality, with no (or much weaker) binding to (−)scDNA crossings.

Topoisomerase IV binding on supercoiled DNA

In absence of strong binding of Topo IV to DNA crossings, we examined the effect of Topo IV binding on the extension of a supercoiled DNA molecule. We begin with an 11-kb DNA stretched at a low, constant force ($F = 0.12$ pN) and overwound by 30 turns ($\sigma = 0.03$); in these conditions, the molecule's extension is constant at 0.35 μm. Addition of Topo IV ([Topo IV] = 0.3 nM) leads to a smooth, gradual increase in the DNA's extension (over ≈100 s, see *inset* in Fig. 3 *a*). Thus, Topo IV interacts with supercoiled DNA in the absence of ATP in a way that increases its extension.

To further characterize this interaction we measure the mean steady-state extension of DNA as a function of $\sigma = n/Lk_0$, in the presence of Topo IV and at fixed force ($F = 0.12$ pN). The response of bare DNA to supercoiling is well understood (16). At low forces ($F < 0.4$ pN) the molecule buckles when twisted by $|n| > |n_c|$ turns and forms (+) or (−) plectonemic supercoils which are mirror-images of each other. The extension versus supercoiling curve is thus typically bell-shaped, with a maximum at $\sigma = 0$ (16,17) (see *blue symbols* on Fig. 3 *a*). Interestingly, the extension of a (+) or (−)scDNA is greater in the presence of Topo IV ([Topo IV] = 3 nM; see *red symbols* on Fig. 3 *a*) than in its absence, indicating that Topo IV binding mainly results in the reduction of the size of plectonemic structures. This difference in extension increases with the degree of supercoiling, suggesting that supercoiling promotes enzyme binding to DNA. On the other hand, we observe no significant changes in the DNA's extension at $\sigma = 0$, which is consistent with a weaker interaction of Topo IV with relaxed DNA as compared to supercoiled DNA (20).

We analyzed the slope of these extension-versus-supercoiling curves (in the regime where the molecule forms plectonemes). In the absence of Topo IV, the DNA's extension (at $F = 0.12$ pN) contracts by $\delta l_0 = 70 \pm 3$ nm

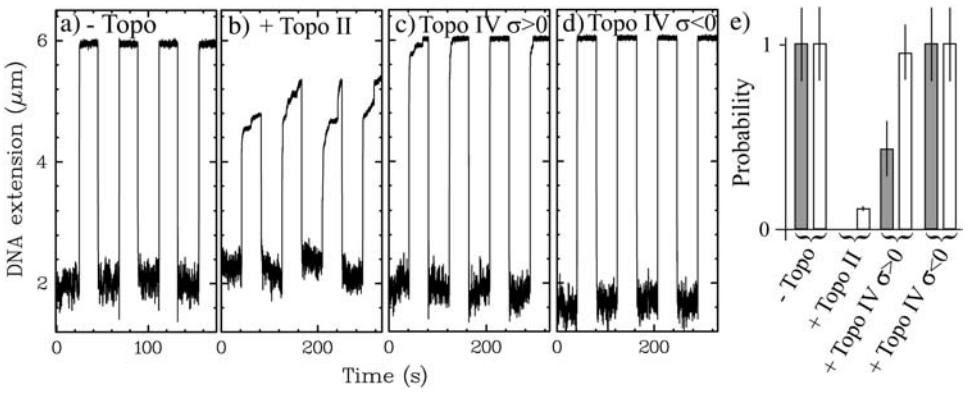

FIGURE 2 Force modulation experiments in the presence of topoisomerase but in the absence of ATP. The extension of a 17-kb scDNA is monitored as the force alternates between low (0.3 pN) and high values (5 pN). In *a–c*, DNA is positively supercoiled ($\sigma = 0.04$), whereas it is negatively supercoiled in *d* ($\sigma = -0.04$). See text for details. (*a*) In the absence of enzyme, alternating between low and high forces yields smooth and reproducible changes in the DNA's extension, corresponding respectively to the appearance and the removal of plectonemic structures. (*b*) In the presence of Topo II, extension plateaus are observed and the full extension at high force is not recovered, a result of the clamping of DNA crossovers by the enzyme (19). Same experiments performed with *E. coli* Topo IV (0.7 nM) on positively supercoiled DNA ($\sigma = 0.04$). Some clamping events are observed, but the full extension at $F = 5$ pN is usually quickly recovered. (*d*) Same experiment as in *c*, but at $\sigma = -0.04$. No clamping events (out of 30) were observed. (*e*) Probability of recovery of the molecule's full extension at $F = 5$ pN: immediately after force increase (*shaded bar*); after 40 s at 5 pN (*open bar*) in the different conditions described in *a–d*).

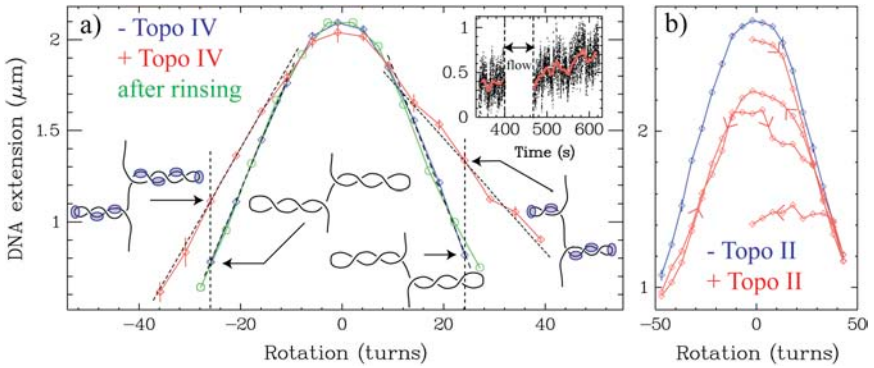

FIGURE 3 Topo IV binding on an 11-kb supercoiled DNA. (*a*, *Inset*) Real-time observation of Topo IV interaction with positively supercoiled DNA. Bare DNA is overwound ($\sigma = 0.03$) and stretched ($F = 0.12$ pN); its extension is constant at 0.35 μm. After addition of Topo IV at a concentration of 0.3 nM (leading to a transient flow in the reaction chamber) the extension gradually increases (timescale ≈100 s), due to the effect of Topo IV binding upon the molecule's extension. Solid dots indicate raw data lowpass filter at 0.05 Hz (*red line*). (*a*, *Main figure*) Mean DNA extension (averaged over five curves) measured in the absence and presence of Topo IV (3 nM) at various number of turns n (i.e., various supercoiling densities). (*Blue points*) Control data obtained in the absence of enzyme (16,17). (*Red points*) Data obtained after injection of 3-nM Topo IV. (*Green points*) Data obtained after washing the reaction chamber. The decrease in extension per added turn was determined using linear fits (*solid dashed lines*) to the appropriate portion of the data. Error bars indicate statistical standard deviation. Schematic shows the typical plectonemic structures expected with or without protein. (*b*) Same experiment in presence of eukaryotic Topo II (≈0.15 nM; $F = 0.45$ pN). After addition of Topo II, successive coiling and uncoiling of the DNA (*arrows* indicate the direction of the acquisition) leads to hysteretic behavior (*red points*), presumably as plectonemic supercoils are locked by the enzyme at some crossings and can no longer be removed by rotating the bead (see also Fig. 2).

with each additional turn of the magnets (positive or negative). In the presence of an excess of enzymes ([Topo IV] > 0.3 nM) the contraction slope is smaller. The slope measured on (+)scDNA $\delta l_p^+ = 31 \pm 1$ nm/turn is different from the one obtained on (−)scDNA, $\delta l_p^- = 48 \pm 1.5$ nm/turn. We thus conclude that Topo IV generates (at forces $F < 0.5$ pN, see Fig. 4, *a* and *b*) tighter plectonemic structures than those observed on bare DNA and that it interacts chirally with scDNA. Since the decrease in extension is smaller for (+)scDNA than for (−)scDNA, the binding of Topo IV to scDNA generates compensating negative supercoils. This interaction of Topo IV with supercoiled DNA is qualitatively similar to that of Gyrase (21), with which it is known to share a large homology.

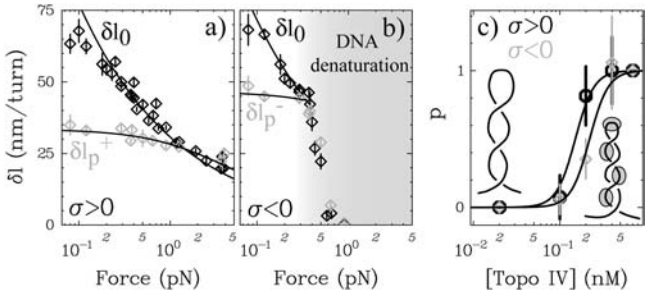

FIGURE 4 (*a*) Decrease in the DNA's extension δl per added turn of the magnets as a function of the force on (+)scDNA in the absence (*solid points*, δl_0) or presence (*shaded points*, δl_p^+) of 3 nM Topo IV. (*b*) Same experiments on (−)scDNA: δl_0 (*solid points*) and δl_p^- (*shaded points*). Above 0.4 pN, (−)scDNA denatures. Error bars indicate the statistical error. The data obtained in the absence of Topo IV were fitted (*solid line*) using a power law (29): $\delta l_0 = AF^{-0.4}$ with $A \approx 30$. The data obtained in the presence of Topo IV were fitted (*solid line*) using the model described in the text with $2\pi R_0 = 40$ nm and $\Delta = 0.16$. (*c*) Probability p of Topo IV binding to scDNA as a function of enzyme concentration (see text for details). Solid circles, (+)scDNA; shaded diamonds, (−)scDNA. Data were collected at $F = 0.2$ pN. The points were fitted using a Hill function (*solid line*).

The analysis of the contraction slopes δl_p^+ and δl_p^-, measured respectively on (+)scDNA and (−)scDNA, as a function of stretching force reveals that they vary little with force (see Fig. 4, *a* and *b*). This observation is in striking contrast with the large variation of δl_0 with force observed on bare DNA. It implies that the plectonemic dimension in the presence of enzyme is not set by the force, as it is for bare scDNA, but is essentially determined by Topo IV binding to scDNA.

The interaction of Topo IV with scDNA is reversible and nonhysteretic: the protein can easily be detached from its substrate by washing the capillary with an enzyme-free buffer (see *green symbols* on Fig. 3 *a*) or by untwisting the DNA to remove its plectonemic supercoils (data not shown). This observation stands in marked contrast with eukaryotic Topo II, where the tight binding of the enzyme to the G- and T-segments results in significant hysteretic behavior upon uncoiling an scDNA (see Fig. 3 *b*) or upon pulling on an scDNA (as discussed above, see Fig. 2).

Measuring the dissociation constant of Topo IV on supercoiled DNA

The enzymatic dissociation constant can be estimated by measuring the slope of contraction δl([Topo IV]) at various concentrations of [Topo IV] to infer the probability p^+ (respectively, p^-) of topoisomerase binding to (+)scDNA (respectively, (−)scDNA). This slope interpolates between δl_0 and δl_p^+ (respectively, δl_p^-). For example, on (+)scDNA, we have $\delta l([\text{Topo IV}]) = p^+ \delta l_p^+ + (1 - p^+)\delta l_0$. This approach has been introduced by Marko and Siggia in their theoretical analysis (22) of the interaction of a protein with a stretched DNA and used by Hegner et al. (23) and Leger et al. (24) to study RecA polymerization on DNA.

The probabilities p^+ and p^- of Topo IV binding to, respectively, (+) and (−)scDNA have thus been measured for

a range of concentration of Topo IV (see Fig. 4 *c*). The binding of Topo IV appears to be cooperative: at a concentration of Topo IV ~0.2 nM, both p^+ and p^- rapidly rise from a very small value to saturation ($p^+ = p^- = 1$). We fitted the binding curves obtained for (+) and (−)scDNA using a Hill function,

$$p = \frac{[\text{TopoIV}]^\alpha}{K_d^\alpha + [\text{TopoIV}]^\alpha}, \quad (4)$$

where $K_d^+ = 0.15 \pm 0.02$ nM for (+)scDNA and $K_d^- = 0.23 \pm 0.02$ nM for (−)scDNA. Despite some large uncertainties (~20%), $\alpha = 4$ yields a good agreement with the data which implies that binding is strongly cooperative. The high binding cooperativity means that for enzymatic concentrations below K_d the probability of having multiple protein complexes bound on DNA is very small, whereas above K_d that probability quickly reaches 100%. The regime below K_d is the regime where we previously observed single enzyme activity in presence of ATP (11).

Dynamics of binding and unbinding at the buckling threshold

We used a small (3-kbp) DNA construct to investigate, with a high signal/noise ratio, the dynamics of Topo IV/DNA interactions. We also used a concentration of Topo IV (3 nM) that was large enough to ensure its quick assembly on plectonemic DNA but not on relaxed (unwrithed) DNA (see below). We twisted the molecule by $n = n'_c = 8$ turns to reach the buckling threshold at $F = 2$ pN (19). As the protein binds to DNA, the molecule buckles to form a loop which is sufficiently long-lived to be observed as a decrease in its extension. Upon protein release the DNA reverts to its full, unbuckled length. The binding/unbinding of protein and DNA therefore results in a characteristic telegraphic signal (see the *middle signal* in Fig. 5 *a*), whereas nothing can be seen at $n = 0 < n'_c$ (*top signal* in Fig. 5 *a*).

The spatial extent of this signal (31 ± 11 nm, see *inset* in Fig. 5 *b*) is equal to the size of a DNA loop at the buckling threshold (≈25 nm, see Fig. 4 *a*), which indicates that one protein is bound per turn. Interestingly, by further rotating the magnets ($n > n'_c$), we were able to detect multiple extension levels, separated by ~30 nm, corresponding to the independent, i.e., noncooperative binding and unbinding of several enzymes (see *bottom signal* in Fig. 5 *a*). This implies that the cooperativity in Topo IV binding to DNA with Hill coefficient $\alpha = 4$ reflects the cooperativity among the enzyme's four subunits, not between different enzymatic complexes.

The duration τ of the looped state gives information on the stability of the protein-DNA complex formed in the absence of ATP. The cumulative probability histogram of this on-time $P(\tau > t)$ ($N = 322$ events) displays a double-exponential behavior characterized by two timescales: 89% of events had an average lifetime of $t_1 = 1.9$ s, and the remaining 11% had an average lifetime of $\sim t_2 = 8.9$ s (see Fig. 5 *b*). Note that, considering the differences between these two timescales and the number of events, it is highly improbable that the times are distributed according to a single exponential. For a single exponential distribution with lifetime t_1 the probability of observing 13 events out of 322 with lifetimes $\geq t_2$ is smaller than 10^{-4}.

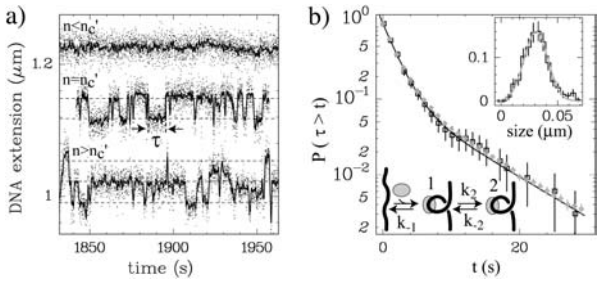

FIGURE 5 Dynamics of Topo IV binding on a short (3 kbp) DNA molecule at 2 pN. (*a*) Traces of DNA extension as a function of time in the presence of Topo IV below ($n = 0 < n_c$, *top trace*), at ($n = 8 = n_c$, *middle trace*) and above the buckling threshold ($n = 10 > n_c$, *bottom trace*). The points are raw data, which are lowpass-filtered (*line*) at 1 Hz. The traces have been vertically shifted to avoid overlapping. From the telegraphic signal, we extracted the size and duration of a binding event. The dashed lines represent the mean change in extension resulting from a single binding event (31 nm, see below). (*b*) Integrated distribution of the duration of binding events (*solid points*) obtained at $n = n_c$ (322 binding times were extracted). The line is a fit using a double exponential: 89% of events had a lifetime $t_1 = 1.9$ s, and the remaining 11% had a lifetime $t_2 = 8.9$ s. (*Shaded points*) Distribution of 10,000 on-times obtained from stochastic simulation of the kinetic pathway drawn in the schematics using the parameters obtained from the fit. Error bars indicate standard deviation. (*Inset*) Histograms of the size of the clamping events. A Gaussian fit gives an average size of 31 nm and a standard deviation of 11 nm. Schematics are two-state binding model of Topo IV on DNA. The distribution of probability of on-times allows us to extract the kinetic parameters k_{-1}, k_2, and k_{-2}(see Materials and Methods).

A similar behavior was reported for the binding of *D. melanogaster* Topo II to DNA (albeit with >10-times longer timescales $t_1 = 20$ s and $t_2 = 260$ s; see Ref. 19). This behavior suggests that the Topo IV/DNA complex can switch rapidly between a weakly bound state *1* and a strongly bound state *2* (see *inset* in Fig. 5). From the cumulative distribution of on-times, we can deduce the kinetic rates of dissociation from state *1* $k_{-1} = 0.48 \pm 0.03\ s^{-1}$, and of switching between states *1* and *2*, $k_2 = 0.03 \pm 0.01\ s^{-1}$ and $k_{-2} = 0.14 \pm 0.01\ s^{-1}$ (see Materials and Methods).

Model for DNA/Topo IV interaction

All the precedent results can be described and quantified by a simple mechanical model of the interaction between Topo IV and DNA, similar to the model introduced by Sarkar and Marko (25).

Loop formation without Topo IV

As any rope, a stretched DNA must be twisted beyond a critical number of turns n_c ($n_c = 36$ turns at $F = 1.9$ pN for an 11-kb DNA) before it buckles to form the plectonemes so common in phone cords. The physical explanation of this phenomenon is pretty standard (26): the larger the force, the more costly the supercoils, in terms of tensional energy. On the other hand, the larger the torque in the molecule, the more favorable they become as plectonemes lower the torsional energy. For a given tension F, there is therefore a critical torque Γ_c (associated to a number of turns n_c) beyond which the torsional energy gained by supercoiling is larger than the cost associated with the plectonemic bending energy and the work against the force performed while supercoiling. At the buckling transition the energetic cost in the formation of a single loop is balanced by the torsional gain. In this mechanical framework, which neglects entropic contributions, the elastic energy of formation of a loop of radius R in a DNA molecule, as in any elastic tube, is (see Fig. 6, *a* and *b*, this article; see also Ref. 27):

$$\mathcal{E}^{\text{loop}} = \left(\frac{B}{2R^2} + F\right) \times 2\pi R. \tag{5}$$

This energy is minimized for a loop of size $R_{\min} = \sqrt{B/(2F)} \approx 7.25\,\text{nm}$ at a force $F = 1.9$ pN (where $B \equiv k_B T \xi$ is the DNA bending modulus, $\xi = 50$ nm its persistence length and $k_B T = 4$ pN · nm, the thermal energy). As just explained the cost of forming that loop: $\mathcal{E}^{\text{loop}} = 4\pi R_{\min} F \approx 43.3\, k_B T$ (see Fig. 6) should be balanced by the torsional work $\mathcal{W}_t$ done twisting the DNA by one additional turn,

$$\mathcal{W}_t = 2\pi\Gamma_c = 4\pi^2 C n_c / L \approx 40\, k_B T, \tag{6}$$

with $C \approx 100$ nm · $k_B T$ the DNA torsional modulus (28) and L=3.6 μm the DNA length. Upon further twisting, plectonemes are formed which lead to a decrease in the molecule's extension δl_0 per added turn. Notice that δl_0 varies inversely with the force: $\delta l_0 \sim F^{-0.4}$ (29), see Fig. 4 *a*).

Loop formation in the presence of Topo IV

In the presence of Topo IV, the buckling transition occurs for a smaller number of turns: $n'_c = 24$ turns (see Fig. 6 *d*), i.e., at a smaller torque Γ'_c. As a wire presenting a local bending defect buckles at that point for a smaller torque than expected, our data suggest that Topo IV locally bends the DNA and thus lowers its buckling threshold. Since we have also seen that Topo IV interacts chirally with DNA, we shall assume that Topo IV bends the G-segment with a radius R_0 and introduces a local change Δ in the DNA writhe ΔWr and twist ΔTw, such that $0 < \Delta = \Delta Wr + \Delta Tw \ll 1$. For example, the bound DNA might wrap in a right-handed way around the enzyme or it might be slightly overtwisted. Since the overall linking number must be conserved (30), Topo IV binding onto DNA a priori induces a compensatory change

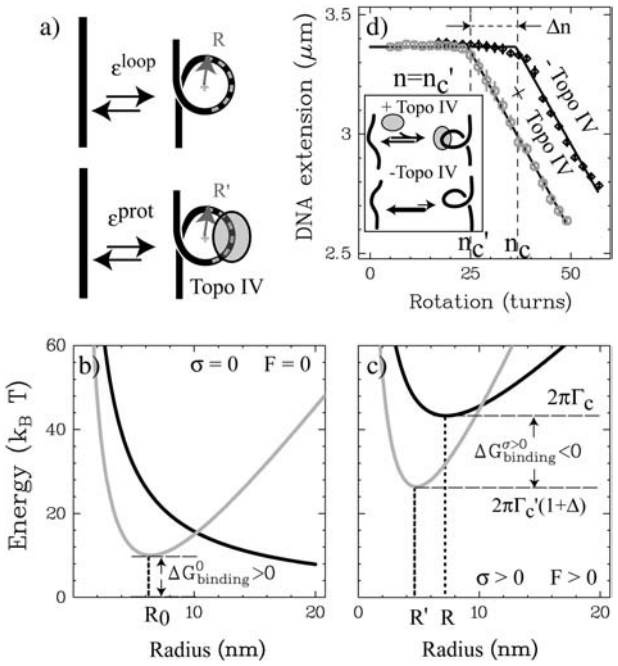

FIGURE 6 Model for DNA/Topo IV interaction at the onset of buckling. (*a*) DNA looping with and without binding of Topo IV. The radius of the loop in the presence of enzyme (R') is, a priori, different than in its absence (R). (*b*) Case $\sigma = 0$ and $F = 0$: in the absence of protein (*solid line*), the bending energy (Eq. 5, with $F = 0$) is minimized for an unbent molecule, $R \to \infty$. In the presence of protein (*shaded line*), the energy (Eq. 7 with $F = 0$), which is minimal for a radius R_0, is larger by $\Delta G^0_{\text{binding}} > 0$ than the energy of the unbent protein free DNA, indicating that enzyme binding on relaxed DNA is not favored. (*c*) Case $\sigma > 0, F > 0$. Same curves as in *b*, but with $F = 1.9$ pN. (Note that this situation also describes the case of a supercoiled circular plasmid, which is always effectively under entropic tension; see Ref. 28.) The relatively large energy of bending at the onset of buckling is balanced by the torsional energy ($2\pi\Gamma_c$). In the presence of protein (*shaded line*), the bending energy is lower than in its absence (*solid line*) by an amount $\Delta G^{\sigma>0}_{\text{binding}} < 0$ (see text) and consequently a smaller torque Γ'_c is required to induce buckling. (*d*) Extension versus rotation data obtained at $F = 1.9$ pN in the absence (*solid diamonds*) or presence (*shaded circles*) of Topo IV (3 nM). Error bars indicate statistical error. The buckling threshold in the absence ($n_c = 36$ turns) or presence ($n'_c = 24$ turns) of Topo IV were obtained using best-fitted piecewise linear functions (*continuous lines*). (*Inset*) At $n = n'_c$, the presence of Topo IV shifts the equilibrium between straight and buckled DNA to the buckled state.

in the Writhe of the rest of the molecule by $-\Delta$ per bound enzyme (the Twist of the unbound supercoiled DNA remains constant after the buckling threshold). Therefore, on (+)scDNA, the number of supercoils is thus reduced upon binding of the enzyme, whereas it is increased on (−)scDNA (see sketch on Fig. 3 *a*). This accounts for the larger contraction slope upon underwinding as compared to overwinding: $\delta l_p^- > \delta l_p^+$.

If binding of Topo IV onto DNA favors a certain radius of bending R_0, then the radius of curvature R of the plectonemic structures formed by DNA in presence of Topo IV will be essentially set by the enzyme, as implied by the data (see Fig. 4, *a* and *b*) and less by the tension on the molecule. At saturating concentrations of Topo IV, the data (see Figs. 3

and 5) also indicate that every added plectonemic turn induces binding of one enzymatic complex. Both observations suggest that at saturating Topo IV concentrations the DNA/enzyme complex adopts the structure shown in the sketches on Figs. 3 and 4 with one complex per plectonemic turn. We can formalize these deductions by writing the energy cost required to form a DNA loop in presence of Topo IV at the onset of buckling (29) as

$$\mathcal{E}^{\text{prot}} = \frac{1}{2}B\left(\frac{1}{R}-\frac{1}{R_0}\right)^2 2\pi R + 2\pi RF + \Delta G^0_{\text{binding}}, \quad (7)$$

(see also Fig. 6). The first term on the right corresponds to the bending energy of a loop of radius R (R_0 is the DNA bending radius at zero force). The second term is the work done against the force F while forming this loop. The third term is the free energy change upon binding of Topo IV onto relaxed DNA ($\sigma = 0$) at $F = 0$. Minimization of $\mathcal{E}^{\text{prot}}$ with respect to R yields the radius R' of the loop at the onset of buckling which is roughly equal to the plectonemes' radius of curvature:

$$R' = \frac{R_0}{\sqrt{1+\dfrac{2FR_0^2}{k_BT\xi}}}. \quad (8)$$

Past the buckling threshold every extra rotation applied to the DNA changes its extension by typically $\delta l_p \sim 2\pi R'$. However, since the interaction of Topo IV with DNA absorbs an amount $\Delta > 0$ of linking number, one needs to rotate the bead clockwise by $1 + \Delta$ turns to actually add one (positive) plectonemic supercoil to the DNA (i.e., to observe a decrease in extension by δl_p). Similarly, one needs to rotate the bead counterclockwise by $1 - \Delta$ turns to add one (negative) plectonemic supercoil to DNA. As a result the DNA's slopes of contraction upon (+) and (−) supercoiling are $\delta l_p^+ = \delta l_p/(1+\Delta)$ and $\delta l_p^- = \delta l_p/(1-\Delta)$.

These considerations account for the experimental data (for both (+) and (−)scDNA; see Fig. 4, *a* and *b*), and yield best-fit values $R_0 = 6.4$ nm and $\Delta = 0.16$ (with an error of 15%). The value of R_0 is close to the Stokes' radius of the enzyme ≈6.5 nm (14). The overwinding of the molecule by $\Delta = 0.16$ (i.e., its binding to negatively supercoiled molecules adds one extra turn for every six turns of unwinding) is comparable to the small (0.06) induction of (+)superhelical turns/Topo IV reported in bulk experiments (14) and recalls the chiral interaction between Gyrase and DNA (15).

Estimating the binding energy of Topo IV onto supercoiled DNA

The data on the binding dynamics of Topo IV, at the buckling threshold $n = n'_c$, suggest that one enzyme binds per DNA loop. As explained previously, at that threshold the cost associated with bending and DNA/protein interaction $\mathcal{E}^{\text{prot}}$ must be balanced by the work $\mathcal{W}'_t$ done by the torque,

$$\mathcal{E}^{\text{prot}} = \mathcal{W}'_t - 2\pi(1+\Delta)\Gamma'_c = 4\pi^2 Cn'_c(1+\Delta)/L \approx 30.9\,k_BT, \quad (9)$$

where the factor $1 + \Delta$ is due to the fact that formation of one loop of DNA around the protein corresponds to $1 + \Delta$ turns of the magnets. Subtracting from the total cost of DNA/protein interaction at the onset of buckling $\mathcal{E}^{\text{prot}}$, the energy of DNA bending (at the same force but in absence of protein) $\mathcal{E}^{\text{loop}}$ yields the free energy of Topo IV binding onto (+)scDNA: $\Delta G^{\sigma>0}_{\text{binding}} = \mathcal{E}^{\text{prot}} - \mathcal{E}^{\text{loop}} \approx -12.3\ k_BT$ (see Fig. 6). This binding free energy is negative, consistent with the observation that Topo IV lowers the threshold for buckling. It agrees with our previous estimate of $K_d^+ = 0.15$ nM and Hill coefficient $\alpha = 4$ for the formation of the enzyme/DNA complex, $\Delta G^{\sigma>0}_{\text{binding}} = -\alpha k_BT \ln([\text{Topo IV}]/K_d^+) = -4\,k_BT \ln(3/0.15) \approx -12\,k_BT$ (where we used the [Topo IV] concentration, 3 nM, at which the binding dynamics has been studied).

From the value of $\mathcal{E}^{\text{prot}}$ and the loop radius $R' \approx 4.8$ nm at $F = 1.9$ pN (Eq. 8), one can also deduce an estimate of the free energy of direct interaction between Topo IV and DNA (at $F = 0$, see Eq. 7): $\Delta G^0_{\text{binding}} \approx 10\,k_BT$. This implies that the dissociation constant of Topo IV on relaxed DNA is $K_d^0 = 3\exp(\Delta G^0_{\text{binding}}/4\,k_BT) \sim 36$ nM, more than two orders-of-magnitude larger than $K_d^{\pm}$. As already reported (10), Topo IV interacts much better with supercoiled than with relaxed DNA (see Fig. 6). Due to the simplistic assumptions that underlie Eq. 7, in particular neglecting fluctuations, we estimate the error on $\Delta G^0_{\text{binding}}$ to be similar to the discrepancy in the estimate of $\mathcal{E}^{\text{loop}}$, i.e., $\sim 3.3\ k_BT$. This error results in a factor 2 of variation in K_d^0, which is nonetheless consistent with previous bulk estimates (14,10).

DISCUSSION

Using our micromanipulation setup, we have quantitatively investigated the binding of Topo IV onto DNA. A straightforward mechanical model of the Topo IV/DNA complex (31,25) allows us to extract many of the parameters characterizing this interaction, such as the radius and local change in linking number of the DNA in the complex, the free energy, and the critical torque at buckling.

From our measurements, we extracted the dissociation constant K_d of the Topo IV/scDNA complex and found that it was slightly smaller for (+) than for (−)scDNA ($K_d^+ = 0.15$ nM and $K_d^- = 0.23$ nM), probably reflecting the chiral interaction of Topo IV with DNA. This binding affinity to supercoiled DNA is approximately two orders-of-magnitude larger than on relaxed DNA. The measured values of K_d are (within a factor 2) similar to previous bulk estimates: $K_d^- \sim 0.6$ nM and $K_d^0 \sim 9.3$ nM (14) (although bulk values as high as $K_d^- \sim 22$ nM, see Ref. 20, have also been reported). The small values of the measured dissociation constant suggest that in bacteria the Topo IV/DNA complex is very stable (a single unbound Topo IV in *E. coli* corresponds to

a concentration ~ 1 nM $> K_d$). The large cooperativity (Hill coefficient $\alpha \approx 4$) of Topo IV binding on DNA has not been reported before (though cooperative binding of gyrase on DNA was observed; see Ref. 32). It is probably due to the fact that the enzyme is a heterotetramer ($ParE_2ParC_2$) whose subunits ParE and ParC assemble cooperatively onto DNA. The ParC and ParE subunits have been observed in solution as dimers and monomers, respectively (33), albeit at a concentration of ~ 100 nM $\gg K_d$. It is thus probable that at the concentrations used here they both appear as monomers that coassemble onto DNA. That explanation is further supported by the agreement between the estimated free energy of binding of Topo IV on (+)scDNA $\Delta G^{\sigma>0}_{\text{binding}}$ and the independently measured value of $K_d^+ = 0.15$ nM for the cooperative assembly of its subunits (in our experiments we used equimolar concentrations of ParE and ParC). The alternative explanation that the observed cooperativity results from interactions between preassembled enzymes is ruled out by the absence of hysteretic behavior in the extension versus supercoiling curves (Fig. 3) and the observation of distinct binding/unbinding events of independent single enzymatic complexes on supercoiled DNA (Fig. 5).

The binding of the bacterial Topo IV onto DNA appears to be very different from that of the eukaryotic Topo II. First, whereas the simultaneous interaction of Topo IV with both the G- and T-segment is weak and reversible (in absence of ATP), Topo II forms a strong and largely irreversible complex with both DNA segments. This difference is manifest in the strong stabilization of DNA crossings by Topo II observed when trying to pull out plectonemes (either by increasing the force or reducing the twist). Second, Topo IV, like Gyrase, but unlike Topo II, bends and wraps or overtwists DNA. Whereas small changes in Writhe or Twist upon binding ($\Delta = 0.16$) are easily detectable with our apparatus, cyclization experiments (12) that observed DNA bending (with a simulated radius $R_0 \sim 7$ nm, similar to the value reported here) were not sensitive enough to detect the chiral interaction of Topo IV with DNA.

The differences in the binding properties of Topo II and Topo IV are striking, given the homology in structure and function of the two enzymes. They could be due to subtle differences in the contacts they make with DNA. Topo IV, like Gyrase, appears to have a more extended bending and wrapping interaction with the G-segment than Topo II, and a weaker interaction with the T-segment (in the absence of ATP). The mechanism of Topo IV binding onto DNA could be closer to that suggested for Gyrase (13). Recent crystallographic data and fluorescence resonance energy transfer studies have shown that the C-terminal domain of GyrA (one of the two subunits of gyrase) and the homologous domain in ParC sharply bend DNA (13). This domain, which is not found in eukaryotic topoisomerases, might be involved in the bending and right-handed wrapping of DNA observed for both Gyrase and Topo IV.

Despite these differences, Topo IV, like Topo II, forms a complex with DNA that can adopt two different states with distinct lifetimes. These states might reflect different structural conformations of the protein with the T-segment, the G-segment or both. It will be interesting to investigate the effect on the lifetime of these states of nonhydrolyzable analogs of ATP (that should affect mostly the interaction of the protein with the T-segment) and of Mg^{2+} ions (that affect the covalent binding of topoisomerases with the G-segment).

The estimate of the free energy of binding of Topo IV onto relaxed DNA, $\Delta G^0_{\text{binding}}$, although consistent with bulk data (14,10), raises a question: how can Topo IV be an efficient decatenase during replication if it has to bind to the two relaxed daughter DNA molecules? A possible solution to that puzzle is suggested by the intertwining of the two molecules, which results in their bending. If the curvature of the braided DNAs is large enough (radius $R < 15$ nm, see Fig. 6 *b*) then binding of Topo IV on these braids may actually lower their free energy.

As a final remark, we note that the approach presented here is very general and could be applied to the study of other protein/DNA complexes that affect the molecule's extension by bending and/or twisting it.

We acknowledge N. Crisona and N.R. Cozzarelli (University of California, Berkeley) for the gift of the *E. coli* Topo IV. We also thank M.-N. Dessinges, G. Lia, and J.-F. Allemand for DNA constructs. We are grateful to O.A. Saleh, K.C. Neuman, and A. Vologodskii for careful reading of the manuscript and helpful discussions and suggestions.

This work was supported by grants from Association pour la Recherche sur le Cancer, Centre National de la Recherche Scientifique, Ecole Normale Supérieure, Universities Paris VII and VI, and a MolSwitch grant from the European Union. G.C. is now funded by the Human Frontier Science Program.

REFERENCES

1. Wang, J. C. 1998. Moving one DNA double helix through another by a type II DNA topoisomerase: the story of a simple molecular machine. *Q. Rev. Biophys.* 31:107–144.
2. Champoux, J. J. 2001. DNA topoisomerases: structure, function, and mechanism. *Annu. Rev. Biochem.* 70:369–413.
3. Roca, J., and J. C. Wang. 1992. The capture of a DNA double helix by an ATP-dependent protein clamp: a key step in DNA transport by type II DNA topoisomerase. *Cell.* 71:833–840.
4. Wang, J. C. 2002. Cellular roles of DNA topoisomerases: a molecular perspective. *Nat. Rev. Mol. Cell Biol.* 3:430–440.
5. Reece, R. J., and A. Maxwell. 1991. DNA gyrase: structure and function. *Crit. Rev. Biochem. Mol. Biol.* 26:335–375.
6. Revyakin, A., R. H. Ebright, and T. R. Strick. 2004. Promoter unwinding and promoter clearance by RNA polymerase: detection by single-molecule DNA nanomanipulation. *Proc. Natl. Acad. Sci. USA.* 101:4776–4780.
7. Hiasa, H., and K. J. Marians. 1994. Topoisomerase IV can support oriC DNA replication in vitro. *J. Biol. Chem.* 269:16371–16375.
8. Zechiedrich, E. L., and N. R. Cozzarelli. 1995. Roles of topoisomerase IV and DNA gyrase in DNA unlinking during replication in *Escherichia coli*. *Genes Dev.* 9:2859–2869.

9. Crisona, N., T. R. Strick, D. Bensimon, V. Croquette, and N. Cozzarelli. 2000. Preferential relaxation of positively supercoiled DNA by *E. coli* topoisomerase VI in single-molecule and ensemble measurements. *Genes Develop.* 14:2881–2892.

10. Stone, M. D., Z. Bryant, N. J. Crisona, S. B. Smith, A. Vologodskii, C. Bustamante, and N. R. Cozzarelli. 2003. Chirality sensing by *Escherichia coli* topoisomerase IV and the mechanism of type II topoisomerases. *Proc. Natl. Acad. Sci. USA.* 100:8654–8659.

11. Charvin, G., V. Croquette, and D. Bensimon. 2003. Single molecule study of DNA unlinking by eukaryotic and prokaryotic type II topoisomerases. *Proc. Natl. Acad. Sci. USA.* 100:9820–9825.

12. Vologodskii, A. V., W. Zhang, V. V. Rybenkov, A. A. Podtelezhnikov, D. Subramanian, J. D. Griffith, and N. R. Cozzarelli. 2001. Mechanism of topology simplification by type II DNA topoisomerases. *Proc. Natl. Acad. Sci. USA.* 98:3045–3049.

13. Corbett, K. D., R. K. Shultzaberger, and J. M. Berger. 2004. The C-terminal domain of DNA gyrase A adopts a DNA-bending β-pinwheel fold. *Proc. Natl. Acad. Sci. USA.* 101:7293–7298.

14. Peng, H., and K. J. Marians. 1995. The interaction of *Escherichia coli* topoisomerase IV with DNA. *J. Biol. Chem.* 270:25286–25290.

15. Kampranis, S. C., A. D. Bates, and A. Maxwell. 1999. A model for the mechanism of strand passage by DNA gyrase. *Proc. Natl. Acad. Sci. USA.* 96:8414–8419.

16. Strick, T., J. F. Allemand, D. Bensimon, A. Bensimon, and V. Croquette. 1996. The elasticity of a single supercoiled DNA molecule. *Science.* 271:1835–1837.

17. Strick, T., J.-F. Allemand, D. Bensimon, and V. Croquette. 1998. The behavior of supercoiled DNA. *Biophys. J.* 74:2016–2028.

18. Zechiedrich, E. L., and N. Osheroff. 1990. Eukaryotic topoisomerases recognize nucleic acid topology by preferentially interacting with DNA crossovers. *EMBO J.* 9:4555–4562.

19. Strick, T. R., V. Croquette, and D. Bensimon. 2000. Single-molecule analysis of DNA uncoiling by a type II topoisomerase. *Nature.* 404: 901–904.

20. Hiasa, H., and K. J. Marians. 1996. Two distinct modes of strand unlinking during θ-type DNA replication. *J. Biol. Chem.* 271:21529–21535.

21. Levine, C., H. Hiasa, and K. Marians. 1998. DNA gyrase and topoisomerase IV: biochemical activities, physiological roles during chromosome replication, and drug sensitivities. *Biochim. Biophys. Acta.* 1400:29–43.

22. Marko, J. F. 1997. Stretching must twist DNA. *Europhys. Lett.* 38: 183–188.

23. Hegner, M., S. B. Smith, and C. Bustamante. 1999. Polymerization and mechanical properties of single RecA-DNA filaments. *Proc. Natl. Acad. Sci. USA.* 96:10109–10114.

24. Léger, J. F., J. Robert, L. Bourdieu, D. Chatenay, and J. F. Marko. 1998. RecA binding to a single double-stranded DNA molecule: a possible role of DNA conformational fluctuations. *Proc. Natl. Acad. Sci. USA.* 95:12295–12296.

25. Sarkar, A., and J. F. Marko. 2001. Removal of DNA-bound proteins by DNA twisting. *Phys. Rev. E.* 64:061909.

26. Landau, L., and E. Lifchitz. 1967. Theory of Elasticity. Mir Editions, Moscow.

27. Strick, T. R., M.-N. Dessinges, G. Charvin, N. H. Dekker, J.-F. Allemand, D. Bensimon, and V. Croquette. 2003. Stretching of macromolecules and proteins. *Rep. Prog. Phys.* 66:1–45.

28. Charvin, G., T. R. Strick, J.-F. Allemand, V. Croquette, and D. Bensimon. 2004. Twisting DNA: single molecules studies. *Contemp. Phys.* 45:383–403.

29. Strick, T. R., G. Charvin, N. H. Dekker, J.-F. Allemand, D. Bensimon, and V. Croquette. 2002. Tracking enzymatic steps of DNA topoisomerases using single-molecule micromanipulation. *C. R. Phys.* 3: 595–618.

30. White, J. H. 1969. Self-linking and the Gauss integral in higher dimensions. *Am. J. Math.* 91:693–728.

31. Marko, J. F., and E. D. Siggia. 1997. Driving proteins off DNA using applied tension. *Biophys. J.* 73:2173–2178.

32. Klevan, L., and J. C. Wang. 1980. DNA gyrase-DNA complex containing 140 base pairs of DNA and an $\alpha_2\beta_2$ protein core. *Biochemistry.* 19:5229–5234.

33. Peng, H., and K. J. Marians. 1993. *Escherichia coli* topoisomerase IV—purification, characterization, subunit structure and subunit interactions. *J. Biol. Chem.* 268:24481–24490.